The Journal of Infectious Diseases

MAJOR ARTICLE

The Influence of Simulated Sunlight on the Inactivation of Influenza Virus in Aerosols

Michael Schuit, Sierra Gardner, Stewart Wood, Kristin Bower, Greg Williams, Denise Freeburger, and Paul Dabisch

National Biodefense Analysis and Countermeasures Center, Operated by BNBI for the US Department of Homeland Security Science and Technology Directorate, Frederick, MD, USA

Background. Environmental parameters, including sunlight levels, are known to affect the survival of many microorganisms in aerosols. However, the impact of sunlight on the survival of influenza virus in aerosols has not been previously quantified.

Methods. The present study examined the influence of simulated sunlight on the survival of influenza virus in aerosols at both 20% and 70% relative humidity using an environmentally controlled rotating drum aerosol chamber.

Results. Measured decay rates were dependent on the level of simulated sunlight, but they were not significantly different between the 2 relative humidity levels tested. In darkness, the average decay constant was 0.02 ± 0.06 min^{-1}, equivalent to a half-life of 31.6 minutes. However, at full intensity simulated sunlight, the mean decay constant was 0.29 ± 0.09 min^{-1}, equivalent to a half-life of approximately 2.4 minutes.

Conclusions. Short-range aerosol transmission of the virus may be possible in full intensity sunlight, but the virus would be unlikely to survive in an infectious state over long distances. These results are consistent with epidemiological findings that sunlight levels are inversely correlated with influenza transmission, and they can be used to better understand the potential for the virus to spread under varied environmental conditions.

Keywords. influenza virus; aerosol; sunlight; relative humidity; decay.

Influenza viruses are significant contributors to the global burden of infectious disease, with estimates of up to 650 000 annual human deaths worldwide linked to respiratory influenza-associated disease alone [1]. Influenza transmission is thought to occur through multiple pathways, including by direct contact with contaminated fluids or surfaces and by aerosols. Transmission via aerosols facilitates the rapid spread of the virus and contributes to its status as both a seasonal and pandemic public health threat for human and susceptible animal populations. Influenza's spread by aerosols has been suggested by epidemiological analyses of transmission patterns, by indoor and outdoor air sampling, by transmission studies with animal models, and by direct measurement of the breath and coughs of infected individuals [2–11].

Viruses in aerosols in both indoor and outdoor environments are subject to environmental stressors, including temperature, relative humidity (RH), and sunlight that may result in losses of infectivity before the virus reaching a host. The decay rate, or rate at which these losses occur, is dependent on the specific phenotype of the virus, composition of the particles containing the virus, and conditions in the surrounding environment. Understanding the effect of these parameters on a virus's decay rate can provide insight into the potential for aerosol transmission to occur in particular environments. Laboratory studies with influenza viruses have indicated that the virus decays slowest at low temperatures and in the absence of ultraviolet (UV) light, with variable effects of RH depending on the composition of the initial suspension liquid [2, 9, 12–15]. These results corroborate epidemiological studies showing higher rates of influenza transmission during winter in temperate regions and either no seasonal variability in the tropics or some increases during rainy seasons [2, 16–18]

However, It is important to note that there are relatively little data on the effect of sunlight on the survival of influenza virus, either alone or in conjunction with other environmental factors. Sunlight has been shown to significantly affect the viability or infectivity of a variety of microorganisms and viruses [19–22], with effects primarily mediated through damage to the genome. Several studies have examined the effects of UVC light on influenza virus as a method of decontamination [12, 23, 24], but UVC light does not penetrate the earth's atmosphere [25], and it is not clear that results from these studies are applicable to understanding the survival of the virus in natural environments. Skinner and Bradish [15] examined the impact of both simulated and real sunlight on influenza virus in liquid aliquots, but they did not measure the impact of these factors on the virus in

Received 6 September 2019; editorial decision 30 October 2019; accepted 18 November 2019; published online November 28, 2019.

Presented in part: American Association for Aerosol Research (AAAR), Portland, Oregon, 17 October 2019.

Correspondence: Michael A. Schuit, MS, 8300 Research Plaza, Frederick, MD 21702 (michael.schuit@nbacc.dhs.gov).

The Journal of Infectious Diseases® 2019;XX:1–7

© The Author(s) 2019. Published by Oxford University Press for the Infectious Diseases Society of America. All rights reserved. For permissions, e-mail: journals.permissions@oup.com.

DOI: 10.1093/infdis/jiz582

Downloaded from https://academic.oup.com/jid/advance-article-abstract/doi/10.1093/infdis/jiz582/5645407 by Boston University user on 30 November 2019

aerosols. Therefore, the aim of the present study was to examine the influence of sunlight and RH on the decay of influenza virus in aerosols.

METHODS

Virus and Assay

Madin-Darby canine kidney (MDCK) cells were used for all virus propagation and quantification. Cells were grown at 37°C with 5% CO_2 in culture media for growth (gMEM) consisting of Minimum Essential Medium ([MEM] Gibco) with 10% heat-inactivated fetal bovine serum ([FBS] Atlanta Biologicals), 2 mM GlutaMAX (Gibco), 0.1 mM nonessential amino acid ([NEAA] Gibco), 1 mM sodium pyruvate (Gibco), and 1% antibiotic-antimycotic solution (Gibco).

Influenza A virus (H1N1) A/PR/8/34 was obtained from the American Type Culture Collection and passaged once in MDCK cells. For stock production, gMEM was removed from confluent monolayers of MDCK cells in T150 flasks. The cells were washed once with phosphate-buffered saline (PBS) and refed with infection media (iMEM), consisting of MEM supplemented with 2 mM GlutaMAX, 0.1 mM NEAA, 1 mM sodium pyruvate, 1% antibiotic-antimycotic solution, 0.2% bovine serum albumin (Sigma-Aldrich), and 0.002 mg/mL TPCK-trypsin (Worthington Biochemical Corp.). Influenza virus was then added to the cells at a multiplicity of infection of 0.001. Once cytopathic effect (CPE) was observed to be greater than 75% at 3 days postinfection, the supernatant containing virus was removed, centrifuged at 4°C for 5 minutes at 360 ×*g* to remove cellular debris, aliquoted, and stored at −80°C until use. For aerosol tests, aliquots were thawed, diluted 1:5 in gMEM, and used within 3 hours.

Concentrations of infectious virus in samples were assessed by microtitration assay in 96-well plates. In brief, gMEM was removed from confluent monolayers of cells in 96-well plates, the cells washed once with PBS, and refed with iMEM. Samples to be assayed were then loaded on the plate, and serial 4-fold dilutions of test samples were performed using a Precision Microplate Pipetting System (BioTek). Plates were incubated at 37°C and 5% CO_2, and visual inspection for CPE was performed 3–4 days postinfection. Viral titers were calculated using the method of Kärber and Spearman [26, 27].

Test System

Decay tests were conducted in a 208-L rotating drum chamber similar to that described by Goldberg et al [28] (Figure 1), but with the added ability to expose aerosols in the chamber to controlled levels of temperature, RH, and simulated sunlight. Air temperature in the chamber is maintained by heating or cooling the walls of the chamber by circulating a temperature-controlled glycol solution through a series of channels in the chamber's shell. All air entering the drum originates from an oil-free compressed air system, in which the air is dehumidified and HEPA filtered. The RH of the air stream is adjusted by passing a portion of the total flow through a Nafion tube bundle. Relative humidity in the drum is brought to near the target value before initiating aerosol generation and fine-tuned by adjustments to the ratio of dry and humid air entering the drum during aerosol generation and sampling procedures. Temperature and RH levels were continuously monitored during tests with a Vaisala HMP110 probe within the drum.

Simulated sunlight originates from a Xenon Arc lamp (Osram GmbH) external to the chamber, with the spectrum shaped by optical filters before entering the chamber through a fused silica window comprising the entirety of one face of the drum. The power setting and light filters used for the solar simulator were selected to produce a spectrum inside the chamber approximating the ASTM G177-03 standard spectrum [29], a reference standard spectrum for UV light exposure based on the Simple Model of the Atmospheric Radiative Transfer of Sunshine (SMARTS). For some tests, the light delivered to the chamber was reduced to 50% intensity by use of a neutral density light filter and adjustments to the lamp power supply.

Spectral irradiance measurements were performed outside the chamber and corrected for window transmission losses using a Gooch & Housego model OL756 spectroradiometer equipped with a model IS-270 2-inch diameter integrating sphere light receptor over the wavelength range from 200 to 800 nanometers. Although the G-177-03 standard itself does not extend above 400 nm, at longer wavelengths the solar simulator output remained relatively consistent with the model used to derive the standard. Aerosols were introduced into, and sampled from, the chamber through an opening located in an axial rotary union on the face of the drum opposite the fused silica window. Aerosols were generated with a 120 kHz Sono-Tek ultrasonic nozzle operated at 3 W into a stainless steel plenum flowing at 10 L/minutes with dry compressed air and directed into the drum. The target mass median aerodynamic diameter (MMAD) of the aerosols was 4–5 μm, an approximate midpoint of size distributions reported for infectious influenza virus aerosols measured in the exhaled breath and coughs of influenza-infected individuals [6, 7]. For each test, the chamber was filled while rotating at 3 rpm for 4 minutes, at which point aerosol generation was terminated and the chamber's inlet and outlet valves sealed. The aerosol in the chamber was allowed to mix for 1 minute before drawing the first sample from the chamber.

The sampling port of the chamber was fitted with a one-half-inch ID Y-fitting, with one arm of the Y connected to the inlet of an Aerodynamic Particle Sizer ([APS] TSI Inc.) and the other arm connected to a 25-mm gelatin filter (SKC Inc.) in a Delrin filter holder (Pall Corp.). The APS was used to measure aerosol size distributions and mass concentrations at each sampling time point using Aerosol Instrument Manager (Aim) software (version 9.0.0.0; TSI, Inc.). Gelatin filters were used to collect material for infectivity analysis, because they have been shown

Downloaded from https://academic.oup.com/jid/advance-article-abstract/doi/10.1093/infdis/jiz582/5645407 by Boston University user on 30 November 2019

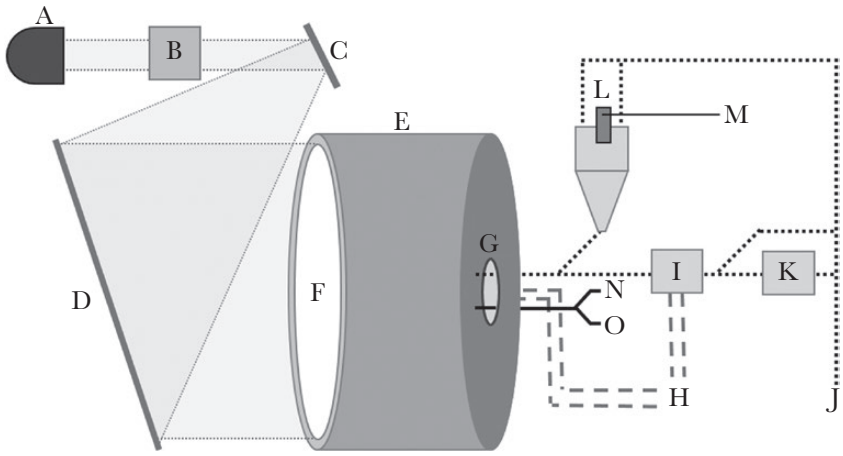

Figure 1. Rotating drum aerosol chamber. The solar simulator's light originates from a Xenon arc lamp (A) and is shaped by a series of optical filters (B) before being redirected by a turning mirror (C) and collimating mirror (D) into the drum itself (E) through a fused-silica window (F). A combined temperature/relative humidity probe is located within the drum on the opposite end, and it is positioned behind a shield (G) to ensure the probe measures the air temperature unbiased by direct radiation from the solar simulator. A temperature-controlled glycol solution (H) is circulated both through the walls of the drum to maintain internal air temperature and through a heat exchanger (I) on the air line into the drum. This line is supplied by dry compressed air (J), which may be conditioned by passing a portion of the flow through a Nafion tube bundle (K) to increase the humidity of the air stream. To fill the drum, air is directed to a plenum housing a 120 kHz ultrasonic nozzle (L) fed by a syringe pump (M). Samples are pulled from the drum through a single line, bifurcated to direct air to both an Aerodynamic Particle Sizer ([APS] N) and gelatin filter (O).

to collect with near 100% physical efficiency and have been used to collect influenza virus aerosols in previous studies [9, 30–32]. Filters were supplied with vacuum flow regulated by a critical flow orifice (O'Keefe Controls Co.). Before use, the flow through each filter was measured with a TSI model 4140 mass flow meter. The mean airflow through the filters across all tests was 5.04 L/minutes with a standard deviation (SD) of ±0.19 L/minutes. After sampling, material collected on gelatin filters was recovered by dissolving the filter in 10 mL gMEM at 37°C.

Six samples were taken over the course of each test, with total test durations ranging from 10 to 40 minutes depending on the environmental condition. At each sampling time point, the sampling port was opened, and aerosols from the drum were sampled by both the APS and the gelatin filter simultaneously for a period of 1 minute, with clean, RH-conditioned air allowed to enter the drum through the inlet to maintain neutral pressure. The airflow, diameter, and length of the tubing on either side of the split were identical. Therefore, it is expected that the size distribution and mass concentration measured by the APS was representative of the aerosols sampled by the filters during the same period.

Decay tests were conducted at 5 separate combinations of environmental conditions, with 5–7 replicate tests at each condition. All tests were conducted at 20°C, because this value approximates room temperature and has been used in other influenza persistence studies [14, 33–35]. Target RH levels of 20% and 70% were selected because previous studies have reported differences in the persistence of influenza virus under these conditions [2, 3, 14, 35]. At low RH levels, persistence tests were conducted in darkness and at half and full intensity simulated sunlight levels. However, application of simulated sunlight introduces additional thermal energy to the rotating drum, and to maintain target air temperature it is necessary to cool the chamber walls to remove that energy from the system. Because of this, it was not possible to achieve high RH values when full intensity sunlight was applied, because the water in the air condenses on the cooler walls. Therefore, only dark conditions and half intensity simulated sunlight could be tested at high RH levels.

Data Analysis

For each test, the mean and SD of each environmental parameter were calculated from all data points starting from the end of aerosol generation to the end of the last aerosol sample. Aerosol concentrations of infectious influenza virus at each sample time point were calculated according to Equation 1. One-phase exponential decay constants were calculated using GraphPad Prism (version 6.03; GraphPad Software, Inc.) from time-series viral aerosol concentrations and aerosol mass concentrations reported by the APS. The decay constant calculated from the virus concentrations represents the total decay rate of particles in the chamber (k_{Total}), and it represents losses due both to physical processes, such as impaction on surfaces and removal of material during sampling, and to loss of viral infectivity over time. The APS measures particle concentration in the chamber, but it does not discriminate between those particles that contain infectious virus and those that do not. Therefore, the decay constant calculated from the APS concentration data represents the physical decay of particles in the chamber ($k_{Physical}$), including dilution of suspended aerosol during sampling intervals. The biological decay constant $k_{Biological}$ for each test was calculated by subtracting the physical decay constant from the total decay

Downloaded from https://academic.oup.com/jid/advance-article-abstract/doi/10.1093/infdis/jiz582/5645407 by Boston University user on 30 November 2019

constant. This term describes the rate of infectivity loss measured in a test, isolated from system-specific physical losses, and was the metric of interest in the present study.

$$C_a = \frac{C_s \cdot \quad V_s}{Q_s \cdot \quad t_s}$$

Equation 1. The measured aerosol concentration (C_a) is the concentration of infectious virus in the air of the test chamber, where C_s is the concentration of material in the sampler medium, V_s is the volume of the sampler medium, Q_s is the sampler flow rate, and t_s is the duration of the sampling period.

The variability of results from different environmental conditions was assessed using a Bartlett's test in GraphPad Prism, and biological decay constants and the mean RH and light intensity values for each test were fit with a generalized linear model (GLM) using JMP v.11.2.0 assuming normal distributions and using an Identity Link Function. A 1-sample *t* test was used to assess whether the mean biological decay constants from different environmental conditions were significantly different than zero (ie, no decay) in GraphPad Prism. A paired *t* test was used to compare the initial and final MMAD values measured by the APS from all tests. All values are reported as arithmetic mean ± SD.

RESULTS

Across all tests, the average temperature was 20.3°C, and the average RH values for low and high RH tests were 20.1% and 69.2% RH, respectively. No test had a temperature SD >0.2°C or RH SD >2.5% RH. At 100% intensity, the simulated sunlight spectrum did not capture the fine detail of the peaks and valleys corresponding to absorption by atmospheric constituents, but it matched the overall trend of the ASTM G-177-03 standard (Figure 2). The integrated UVA and UVB levels for the spectra at 100% intensity were 52.86 and 1.44 W/m^2, respectively, with corresponding values of 24.48 and 0.62 W/m^2 at 50% intensity. Integrated UVC light levels are not reported, because the G-177-03 standard does not include any specifications for light intensities below 280 nm, and measured values did not rise above the limit of detection of the spectroradiometer.

Decay tests were conducted at 5 separate conditions, with resulting k-values shown in Figure 3. Decay rates were significantly influenced by light intensity, but not RH, although the data were more variable at higher RH. Physical and total decay curves from a representative test are shown in Figure 4A. The average R^2 value for the physical decay curve fits measured with the APS across all tests was 0.99 ± 0.01. The average R^2 value for curve fits from viral concentration data for tests with simulated sunlight and in darkness were 0.89 ± 0.10 and 0.51 ± 0.29, respectively. The mean biological decay constants for the latter set were not significantly different than zero (P = .24), and the

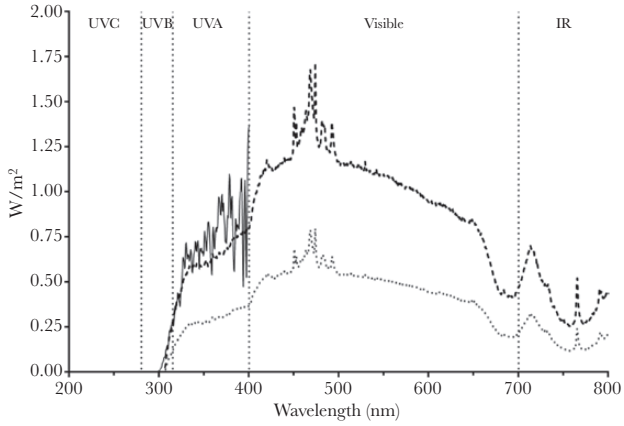

Figure 2. ASTM G-177-03 standard spectrum and representative spectra from the solar simulator. Solid tracing shows the ASTM G-177-03 standard, dashed tracing shows the 100% intensity spectrum from the present study, and dotted tracing shows the 50% intensity spectrum.

low R^2 values for these tests are reflective of the fact that the exponential decay model offers little predictive value over simply taking the mean of the sample titers within each test.

Parametric analyses were not applicable to the biological decay constants for these tests, because there was unequal variance across conditions (P = .0073). Therefore, a GLM was used to test the effects of both parameters and any potential interactions. This analysis found that light intensity had a significant effect on decay rate (P < .0001), but RH and the interaction between RH and light intensity were not significant factors (P = .2643 and P = .9196, respectively).

Across all tests, the starting and final MMAD were 4.4 ± 0.2 μm and 4.1 ± 0.2 μm, respectively. The starting and final geometric SD were 1.32 ± 0.02 and 1.34 ± 0.04, respectively. Although the size distributions remained within in the target range of 4–5 μm throughout the duration of each test, as

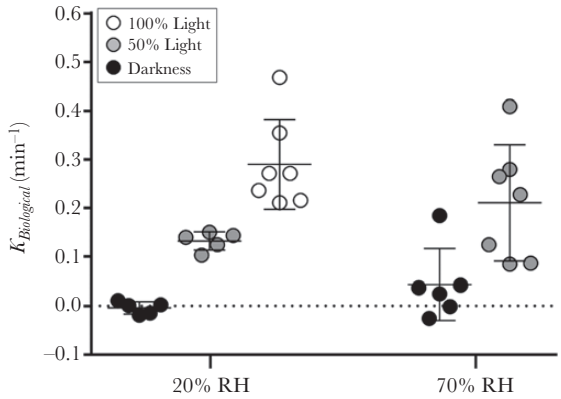

Figure 3. Decay test results. Tests were conducted at 20°C with the PR8 strain of influenza A virus at 20% and 70% relative humidity (RH) and 3 light conditions. A generalized linear model of results demonstrated that simulated sunlight had a significant effect on decay rate (P < .0001), but RH and the interaction between RH and simulated sunlight did not (P = .2643 and P = .9196, respectively).

Downloaded from https://academic.oup.com/jid/advance-article-abstract/doi/10.1093/infdis/jiz582/5645407 by Boston University user on 30 November 2019

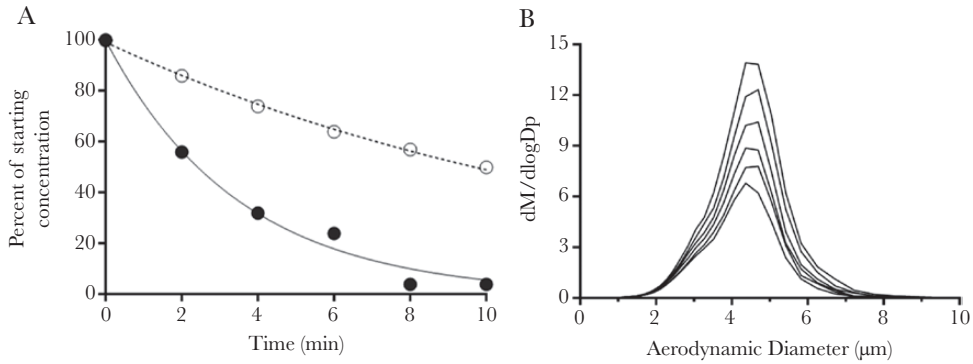

Figure 4. Decay and size data from a representative test. Data are from a test at 20% relative humidity and 100% light intensity. (A) The total aerosol mass (white) and infectious virus concentrations (black) are shown as a percentage of their starting concentration on the first sample of the test. (B) Particle size distributions from top to bottom are from Aerodynamic Particle Sizer (APS) measurements taken at t = 0, 2, 4, 6, 8, and 10 minutes after aerosol loading of the rotating drum aerosol chamber.

shown in APS tracings from a representative test in Figure 4B, the difference in the initial and final MMAD was statistically significant ($P < .0001$) and represents a 23% reduction in mass for a spherical particle with a diameter equal to the MMAD. Although the infectivity data collected at the end of the decay tests are somewhat biased towards smaller particles compared with data at the beginning of the test, the degree of this bias is relatively small, and no attempts were made to correct for this shift.

DISCUSSION

Seasonal influenza virus is a significant contributor to global rates of infectious disease morbidity and mortality, and the possible threat of pandemic influenza is of great concern to public health officials. Data on the effect of environmental conditions on the decay of influenza virus in aerosols can be useful for understanding the potential for the virus to spread in different environments, and they may aid in efforts to model the spread of the disease during either pandemic or seasonal events. The present study assessed the decay of influenza virus in aerosols as a function of simulated sunlight level and RH at 20°C. Although other studies have reported on the impact of simulated and real sunlight on influenza decay in liquid aliquots or UVC light on influenza decay in aerosols [12, 15], data from the present study represent the first results addressing the influence of a light spectrum representative of natural sunlight on the decay of influenza virus in aerosols. Significant losses of infectivity were not observed in darkness at either 20% or 70% RH. However, decay increased significantly with the addition of simulated sunlight at both RH levels tested. These results suggest that aerosol transmission of the virus is more likely to occur at night, indoors, or in other conditions of reduced sunlight intensity.

Studies on the impact of RH on influenza virus in aerosols have generally found that the biological decay of the virus is near zero in darkness at room temperature and low RH, which is in agreement with the findings of the present study. There is less consensus on the effect of higher humidity levels on influenza decay rates, including levels similar to those tested in the present study [36]. Although some studies have reported maximum decay at mid-level RH values (approximately 50%–70% RH) [14, 34, 37], others have reported maximum decay at high RH values (above approximately 70% RH) [2, 35, 38], with the difference in outcomes possibly resulting from variability in the composition of the initial virus suspension medium [14, 36]. This possibility is bolstered by the results of recent studies on influenza decay in droplets on surfaces, which have demonstrated that the effects of RH are minimized or eliminated by the addition of protein-containing liquids such as FBS, mucus, or bronchiolar epithelial cell extracellular material to the initial virus suspension [9, 14]. In the present study, results from tests at high RH were not significantly different from results at low RH at equivalent light levels, although they were notably more variable at high RH. Culture media with a final concentration of 8% FBS was the only suspension liquid used for these tests, and it is possible that the protein content of this liquid contributed to the observed lack of RH effect. However, the lack of data at 70% RH and 100% light intensity limit the ability to make definitive conclusions regarding the effects of RH and RH-light interactions. Further tests incorporating additional particle compositions and environmental conditions would be necessary to explore the potential effects of these parameters, as well as to identify the reason for the greater variability in decay results at high RH. Furthermore, because data in the present study were generated with a laboratory-adapted strain of influenza virus, additional tests with wild-type viruses would be useful to confirm the applicability of results from the present study to currently circulating strains.

Although no studies have been published on the effect of sunlight or simulated sunlight on decay rate of influenza virus in aerosols, data do exist from UVC inactivation studies and a study that examined the effect of both simulated and real sunlight on influenza decay in liquid suspensions [12, 15, 23, 24].

Downloaded from https://academic.oup.com/jid/advance-article-abstract/doi/10.1093/infdis/jiz582/5645407 by Boston University user on 30 November 2019

These studies demonstrate that decay of the virus increases both with increasing duration of exposure and with higher intensities of light, consistent with results from the present study.

The light spectrum used in the present study was optimized in the UV region to match an ASTM standard that was developed to represent a reasonable upper exposure limit for UV light for weathering applications [29], and it is similar to the spectrum that would be expected under clear skies at noon on the summer solstice for a high-elevation, mid-latitude city. Shorter wavelengths of light (ie, UVA and UVB) have been shown to have exponentially greater impact on the viability of microorganisms than longer wavelengths of light [39, 40]. Therefore, decay data generated using the ASTM G177-03 spectrum are expected to represent a reasonable upper limit estimate for decay of influenza exposed to natural sunlight. Natural outdoor sunlight spectra may have lower intensities than the spectrum used in the preset study depending on geographic location, time of day, and local atmospheric conditions. However, the results from the present study would be expected to bound the range of decay rates that would be expected for temperate regions at equivalent temperature and RH levels.

CONCLUSIONS

The decay rates observed at the maximum light intensity used in the present study suggest that long-range outdoor aerosol transmission of influenza virus would be unlikely to occur during the day under clear-sky conditions. However, aerosol transmission in such conditions could still be possible over short distances and time scales, and any factors leading to lower light intensities would be expected to lead to a corresponding decrease in decay rate and increase in transmission potential. These results are consistent with observed increases of influenza incidence during winter in temperate regions and rainy seasons in the tropics [41, 42], and they may be useful to inform efforts to understand the mechanism behind this correlation.

Notes

Disclaimer. The views and conclusions contained in this document are those of the authors and should not be interpreted as necessarily representing the official policies, either expressed or implied, of the Department of Homeland Security (DHS) or the U.S. Government. DHS does not endorse any products or commercial services mentioned in this document.

Financial support. This work was fully funded under Contract No. HSHQDC-15-C-00064 awarded to Battelle National Biodefense Institute (BNBI) by the Department of Homeland Security Science and Technology Directorate (S&T) for the operation and management of the National Biodefense Analysis and Countermeasures Center (NBACC), a Federally Funded Research and Development Center.

Potential conflicts of interest. At the time the work described in this manuscript was performed, all authors were affiliated with the NBACC, operated by BNBI for the US DHS S&T Directorate. Since that time, 1 author (K. B.) has left the NBACC. All authors have submitted the ICMJE Form for Disclosure of Potential Conflicts of Interest. Conflicts that the editors consider relevant to the content of the manuscript have been disclosed.

References

1. Iuliano AD, Roguski KM, Chang HH, et al.; Global Seasonal Influenza-associated Mortality Collaborator Network. Estimates of global seasonal influenza-associated respiratory mortality: a modelling study. Lancet **2018**; 391:1285–300.
2. Hemmes JH, Winkler KC, Kool SM. Virus survival as a seasonal factor in influenza and polimyelitis. Nature **1960**; 188:430–1.
3. Lowen A, Palese P. Transmission of influenza virus in temperate zones is predominantly by aerosol, in the tropics by contact: A hypothesis. PLOS Currents Influenza **2009**; 1. doi:10.1371/currents.RRN1002.
4. Corzo CA, Culhane M, Dee S, Morrison RB, Torremorell M. Airborne detection and quantification of swine influenza a virus in air samples collected inside, outside and downwind from swine barns. PLoS One **2013**; 8:e71444.
5. Lindsley WG, Blachere FM, Davis KA, et al. Distribution of airborne influenza virus and respiratory syncytial virus in an urgent care medical clinic. Clin Infect Dis **2010**; 50:693–8.
6. Lindsley WG, Blachere FM, Thewlis RE, et al. Measurements of airborne influenza virus in aerosol particles from human coughs. PLoS One **2010**; 5:e15100.
7. Milton DK, Fabian MP, Cowling BJ, Grantham ML, McDevitt JJ. Influenza virus aerosols in human exhaled breath: particle size, culturability, and effect of surgical masks. PLoS Pathog **2013**; 9:e1003205.
8. Brankston G, Gitterman L, Hirji Z, Lemieux C, Gardam M. Transmission of influenza A in human beings. Lancet Infect Dis **2007**; 7:257–65.
9. Kormuth KA, Lin K, Prussin AJ, et al. Influenza virus infectivity is retained in aerosols and droplets independent of relative humidity. J Infect Dis **2018**; 218:739–47.
10. Scoizec A, Niqueux E, Thomas R, Daniel P, Schmitz A, Le Bouquin S. Airborne detection of H5N8 highly pathogenic avian influenza virus genome in poultry farms, France. Front Vet Sci **2018**; 5:15.
11. Jonges M, van Leuken J, Wouters I, Koch G, Meijer A, Koopmans M. Wind-mediated spread of low-pathogenic avian influenza virus into the environment during outbreaks at commercial poultry farms. PLoS One **2015**; 10:e0125401.
12. McDevitt JJ, Rudnick SN, Radonovich LJ. Aerosol susceptibility of influenza virus to UV-C light. Appl Environ Microbiol **2012**; 78:1666–9.

Downloaded from https://academic.oup.com/jid/advance-article-abstract/doi/10.1093/infdis/jiz582/5645407 by Boston University user on 30 November 2019

13. Lowen AC, Mubareka S, Steel J, Palese P. Influenza virus transmission is dependent on relative humidity and temperature. PLoS Pathogens **2007**; 3:e151.
14. Yang W, Elankumaran S, Marr LC. Relationship between humidity and influenza A viability in droplets and implications for influenza's seasonality. PLoS One **2012**; 7:e46789.
15. Skinner H, Bradish C. Exposure to light as a source of error in the estimation of the infectivity of virus suspensions. Microbiology **1954**; 10:377–97.
16. Biswas PK, Islam MZ, Debnath NC, Yamage M. Modeling and roles of meteorological factors in outbreaks of highly pathogenic avian influenza H5N1. PLoS One **2014**; 9:e98471.
17. Chowell G, Towers S, Viboud C, et al. The influence of climatic conditions on the transmission dynamics of the 2009 A/H1N1 influenza pandemic in Chile. BMC Infect Dis **2012**; 12:298.
18. Viboud C, Alonso WJ, Simonsen L. Influenza in tropical regions. PLoS Med **2006**; 3:e89.
19. Rzezutka A, Cook N. Survival of human enteric viruses in the environment and food. FEMS Microbiol Rev **2004**; 28:441–53.
20. Tang JW. The effect of environmental parameters on the survival of airborne infectious agents. J R Soc Interface **2009**; 6 (Suppl 6):S737–46.
21. Nelson KL, Boehm AB, Davies-Colley RJ, et al. Sunlight-mediated inactivation of health-relevant microorganisms in water: a review of mechanisms and modeling approaches. Environ Sci Process Impacts **2018**; 20:1089–122.
22. Qiao Z, Ye Y, Chang PH, Thirunarayanan D, Wigginton KR. Nucleic acid photolysis by UV254 and the impact of virus encapsidation. Environ Sci Technol **2018**; 52:10408–15.
23. Welch D, Buonanno M, Shuryak I, Randers-Pehrson G, Spotnitz HM, Brenner DJ. Far-UVC light applications: sterilization of MRSA on a surface and inactivation of aerosolized influenza virus. Proc. SPIE 10479, Light-Based Diagnosis and Treatment of Infectious Diseases **2018**; 10479:104791D.
24. Jensen MM. Inactivation of airborne viruses by ultraviolet irradiation. Appl Microbiol **1964**; 12:418–20.
25. Christiaens FJ, Chardon A, Fourtanier A, Frederick JE. Standard ultraviolet daylight for nonextreme exposure conditions. Photochem Photobiol **2005**; 81:874–8.
26. Kärber G. [Beitrag zur kollektiven Behandlung pharmakologischer Reihenversuche]. Naunyn-Schmiedebergs Archiv für experimentelle pathologie und pharmakologie **1931**; 162:480–3.
27. Spearman C. The method of 'right and wrong cases'('constant stimuli') without Gauss's formulae. Br J Psychol **1908**; 2:227–42.
28. Goldberg L, Watkins H, Boerke E, Chatigny M. The use of a rotating drum for the study of aerosols over extended periods of time. Am J Hyg **1958**; 68:85–93.
29. ASTM International. G177-03(2012) Standard Tables for Reference Solar Ultraviolet Spectral Distributions: Hemispherical on 37° Tilted Surface. ASTM International **2012**. doi:10.1520/G0177-03R12.
30. Burton NC, Grinshpun SA, Reponen T. Physical collection efficiency of filter materials for bacteria and viruses. Ann Occup Hyg **2006**; 51:143–51.
31. Zuo Z, Kuehn TH, Verma H, et al. Association of airborne virus infectivity and survivability with its carrier particle size. Aerosol Sci Tech **2013**; 47:373–82.
32. Hatagishi E, Okamoto M, Ohmiya S, et al. Establishment and clinical applications of a portable system for capturing influenza viruses released through coughing. PLoS One **2014**; 9:e103560.
33. Pyankov OV, Pyankova OG, Agranovski IE. Inactivation of airborne influenza virus in the ambient air. J Aerosol Sci **2012**; 53:21–8.
34. Schaffer FL, Soergel ME, Straube DC. Survival of airborne influenza virus: effects of propagating host, relative humidity, and composition of spray fluids. Arch Virol **1976**; 51:263–73.
35. Harper GJ. Airborne micro-organisms: survival tests with four viruses. Epidemiol Infect **1961**; 59:479–86.
36. Paynter S. Humidity and respiratory virus transmission in tropical and temperate settings. Epidemiol Infect **2015**; 143:1110–8.
37. Shechmeister IL. Studies on the experimental epidemiology of respiratory infections. III. Certain aspects of the behavior of type A influenza virus as an air-borne cloud. J Infect Dis **1950**; 87:128–32.
38. Noti JD, Blachere FM, McMillen CM, et al. High humidity leads to loss of infectious influenza virus from simulated coughs. PLoS One **2013**; 8:e57485.
39. Munakata N, Saito M, Hieda K. Inactivation action spectra of *Bacillus subtilis* spores in extended ultraviolet wavelengths (50-300 nm) obtained with synchrotron radiation. Photochem Photobiol **1991**; 54:761–8.
40. Mamane-Gravetz H, Linden K. Relationship between physiochemical properties, aggregation and UV inactivation of isolated indigenous spores in water. J Appl Microbiol **2005**; 98:351–63.
41. Tamerius J, Nelson MI, Zhou SZ, Viboud C, Miller MA, Alonso WJ. Global influenza seasonality: reconciling patterns across temperate and tropical regions. Environ Health Perspect **2011**; 119:439–45.
42. Ianevski A, Zusinaite E, Shtaida N, et al. Low temperature and low UV indexes correlated with peaks of influenza virus activity in Northern Europe during 2010–2018. Viruses **2019**; 11:207.

Downloaded from https://academic.oup.com/jid/advance-article-abstract/doi/10.1093/infdis/jiz582/5645407 by Boston University user on 30 November 2019